A Note on the Application of Edge-Elements for Modeling Three-Dimensional Inhomogeneously-Filled Cavities

Jin-Fa Lee, *Member, IEEE,* and Raj Mittra, *Fellow, IEEE*

Abstract—**The application of edge-elements for modeling three-dimensional inhomogeneously-filled cavities is presented in this paper. Explicit representations for the two element matrices, $[S]_e$ and $[T]_e$, are provided in order to facilitate the implementation of the FEM formulation. Also included are the results of a numerical experiment that investigates the rate of convergence of the computation of the dominant resonance frequency of a rectangular cavity when the edge-element formulation is employed.**

I. Introduction

THE ANALYSIS of inhomogeneously-filled cavities is important in many applications, e.g., the design of microwave filters and ovens. For all but a few simplest three-dimensional configurations, this analysis must be carried out numerically. The numerical methods that are available for analyzing three-dimensional cavities are: the transmission line matrix method [1], the finite difference methods [2], and the finite element methods (FEMs) [3], [4]. Among these, FEM offers the most flexibility in modeling cavities with arbitrary geometries as well as with highly inhomogeneous fillings. However, it is well known that the finite element analysis of high-frequency electromagnetic problems is plagued by the occurrence of nonphysical, spurious modes [4].

A number of recent publications have suggested various approaches to eliminating the spurious modes. Rahman and Davies [5] have used a penalty function to enforce the divergence-free condition. The penalty function approach makes the numerical solution depend on a parameter whose precise effect on the solution is often difficult to assess. Kobelansky and Webb [6] proposed the use of divergence-free fields as the bases in the variational procedure. Unfortunately, this approach requires intensive computation time to obtain an accurate solution.

A different approach to eliminating the spurious modes is to use edge-elements [7]. Edge-elements are recently-developed finite-element bases for vector fields, which have the unique property that the degrees of freedom associated with these elements are the circulations of the vector field along the edges of the mesh. With edge-elements, only the tangential continuity of the vector field is imposed across element boundaries. The advantages of edge-elements are: (i) They impose the continuity of only the tangential components of the electric and magnetic fields, which is consistent with the physical constraints on these fields; (ii) The interfacial boundary conditions are automatically obtained through the natural boundary condition in the variational process; and, (iii) Dirichlet boundary condition can be easily imposed along the element edges.

In this paper, we apply the edge-element formulation to the solution of inhomogeneously-filled cavities. The application of edge-elements to modeling three-dimensional cavities has been presented in [8], [9]. Two principal contributions of this paper are: (i) The element matrices for the corresponding variational functional are provided explicitly; and, (ii) The rate of convergence of edge-elements for calculating the resonant frequency of cavities is determined through a numerical experiment for an air-filled rectangular cavity.

The paper is organized as follows: Section II presents the variational formulation of three-dimensional inhomogeneously-filled cavities. The solution procedure of the variational formulation in a finite-dimensional space, or the finite element implementation, is presented in Section III. To perform the convergence study, we need to divide an initial mesh into similar but finer meshes. A simple mesh-division algorithm, which divides a tetrahedron into eight smaller tetrahedra, is presented in Section IV, along with the results of the convergence study for a canonical cavity problem. Numerical results are included in Section V. Finally, a brief conclusion is given in Section VI.

II. Variational Formulation

The basic equations that govern EM fields in source-free, time-harmonic regions are the Maxwell equations

$$\nabla \times \vec{E} = -j\omega\mu\vec{H} \tag{1}$$

Manuscript received September 11, 1991; revised February 19, 1992.

J.-F. Lee is with Department of Electrical Engineering, Worcester Polytechnic Institute, 100 Institute Road, Worcester, MA 01609.

R. Mittra is with the ECE Department, University of Illinois, 1406 West Green Street, Urbana, IL 61801.

IEEE Log Number 9201714.

$$\nabla \times \vec{H} = j\omega\epsilon\vec{E} \tag{2}$$

where ϵ and μ are the permittivity and permeability, respectively. We note that, with $\omega \neq 0$, (1) and (2) imply that

$$\nabla \cdot \mu\vec{H} = 0 \tag{3}$$

$$\nabla \cdot \epsilon\vec{E} = 0 \tag{4}$$

The substitution of $\vec{E}$ from (2) into (1) and of $\vec{H}$ from (1) into (2) yields the vector wave equations:

$$\nabla \times \frac{1}{\mu_r} \nabla \times \vec{E} = k^2\epsilon_r\vec{E} \tag{5}$$

$$\nabla \times \frac{1}{\epsilon_r} \nabla \times \vec{H} = k^2\mu_r\vec{H} \tag{6}$$

where $k^2 = \omega^2\mu_0\epsilon_0$, ϵ_0, μ_0 are the permittivity and permeability of air, respectively. In view of the similarity between (5) and (6), the analysis in this paper will be presented in terms of the electric field $\vec{E}$; the parallel development for the magnetic field $\vec{H}$ is obtained by making the substitutions $\vec{E} \rightarrow \vec{H}$ and $\mu \rightarrow \epsilon$.

It is well known that the field solution in a three-dimensional cavity can be formulated in a variational form [10]. If the cavity contains only lossless materials, the variational functional in terms of $\vec{E}$ can be written as

$$F(\vec{E}) = \int_\Omega \frac{1}{\mu_r} \|\nabla \times \vec{E}\|^2 - k^2\epsilon_r \|\vec{E}\|^2 \, d\Omega. \tag{7}$$

From the functional (7), we note that both $\nabla \times \vec{E}$ and $\vec{E}$ need to be square integrable. Consequently, the solution is sought from the function space $L^2_{\text{curl}}(\Omega)$, which is defined by

$$L^2_{\text{curl}}(\Omega) = \{\vec{E} \in L^2(\Omega): \nabla \times \vec{E} \in L^2(\Omega)\} \tag{8}$$

where $L^2(\Omega)$ is the linear space of square-integrable vector fields defined on the problem domain Ω.

III. Finite-Dimensional Discretization

The variational formulation in the previous section seeks the solution in the function space $L^2_{\text{curl}}(\Omega)$ which is infinite-dimensional. In order to solve a three-dimensional cavity problem on a digital computer, we need to convert the original continuum problem into a discretized version. This can be accomplished by using the finite element method. The basic idea of FEM can be described as follows [7]. First, we formulate the corresponding variational functional and the admissible function space, for example, $L^2_{\text{curl}}(\Omega)$ as in previous section. Then restrict the class to a smaller, finite dimensional function space $W(\Omega)$, which can be described by a finite number of parameters (the degrees of freedom). If this constraint is imposed properly, stationarity will occur at a point which is in the neighborhood of the true solution. Finally, imposition of the stationarity condition leads to a finite number of equations with respect to the degrees of freedom.

The approximate solution $\vec{E}_{\text{app}}$ of (7) in the function space $W(\Omega)$, where $W(\Omega) \subset L^2_{\text{curl}}(\Omega)$, is the stationary point of the functional (7) in $W(\Omega)$ with respect to the variations of $\vec{E}$. Whatever the choice of the function space $W(\Omega)$, the functional $F(\vec{E})$ in $W(\Omega)$ may be expressed in a matrix form as

$$F(\vec{E}) = \frac{1}{2} e^t[S]e - \frac{k^2}{2} e^t[T]e. \tag{9}$$

Here, e is the coefficient vector and the square matrices $[S]$ and $[T]$ are given by

$$[S]_{mn} = \int_\Omega \frac{1}{\mu_r} (\nabla \times \vec{\alpha}_m) \cdot (\nabla \times \vec{\alpha}_n) \, d\Omega \tag{10}$$

$$[T]_{mn} = \int_\Omega \epsilon_r \vec{\alpha}_m \cdot \vec{\alpha}_n \, d\Omega \tag{11}$$

where $\vec{\alpha}_i's$ are the vector functions that are used to span the vector function space $W(\Omega)$.

In the present approach, the problem domain Ω is broken into tetrahedra within which the material properties ϵ_r and μ_r are constant, although they may be discontinuous across the element boundaries. In each tetrahedron, the electric field is expressed as a linear combination of edge-elements, i.e., we write

$$\vec{E} = \sum_{i<j} e_{ij} \vec{w}_{ij} \tag{12}$$

where $\vec{w}_{ij} = \lambda_i \nabla\lambda_j - \lambda_j \nabla\lambda_i$, λ_i is the barycentric function of node i, is the Whitney 1-form associated with *edge* $\{i, j\}$ [7]. The derivations of the element matrices, $[S]_e$ and $[T]_e$, of edge-elements in a tetrahedral mesh is the topic of the next section.

3.1 Element Matrices

In the finite element method, the global matrices $[S]$ and $[T]$ of (9) are the assembly of the element matrices, $[S]_e$ and $[T]_e$, i.e.

$$[S] = \sum_e [S]_e \tag{13}$$

$$[T] = \sum_e [T]_e. \tag{14}$$

The constructions of the element matrices, $[S]_e$ and $[T]_e$ depend on the choice of the finite dimensional function space $W(\Omega)$. In the present approach, $W(\Omega)$ is spanned by edge-elements on a tetrahedral mesh. Shown in Fig. 1 is the configuration of edge-element in a tetrahedron. The geometrical identities that are useful in the derivation, given below are

$$\nabla\lambda_i = \frac{\vec{A}_i}{3V} \tag{15}$$

$$\vec{A}_i \times \vec{A}_j = \frac{3V}{2} s(-1)^{j-i} \vec{t}_{k,l}$$

$$s = \text{sgn}\,(\vec{t}_{1,2} \times \vec{t}_{1,3} \cdot \vec{t}_{1,0}) \tag{16}$$

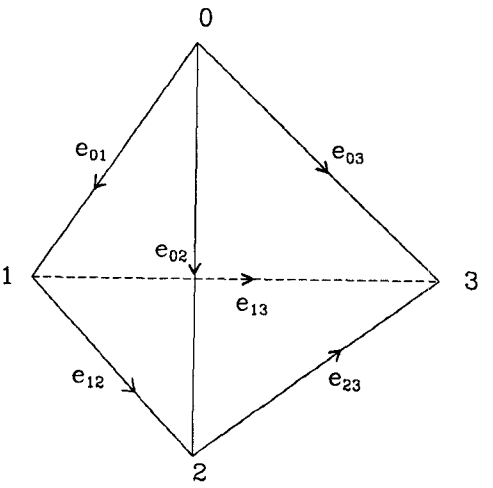

Fig. 1. Edge-element on a tetrahedron.

for $i < j$. Here, $\vec{A}_i$ is the area normal of the triangular face $\{j, k, l\}$ pointing into the tetrahedron, V is the volume of the tetrahedron, $\vec{t}_{k,l}$ is a vector from node k to node l, and $\{k, l\} = \{0, 1, 2, 3\} - \{i, j\}$, with $k < l$. With these identities, $\nabla \times \vec{E}$ can be written as

$$\nabla \times \vec{E} = \frac{2}{9V^2} \sum_{i<j} e_{ij} \vec{A}_i \times \vec{A}_j = \frac{s}{3V} \sum_{i<j} e_{ij} (-1)^{j-i} \vec{t}_{k,l}$$

$$= \frac{s}{3V} [e_{01} \quad e_{02} \quad e_{03} \quad e_{12} \quad e_{13} \quad e_{23}] \begin{bmatrix} -\vec{t}_{2,3} \\ \vec{t}_{1,3} \\ -\vec{t}_{1,2} \\ -\vec{t}_{0,3} \\ \vec{t}_{0,2} \\ -\vec{t}_{0,1} \end{bmatrix}. \tag{17}$$

Finally, the element matrix $[S]_e$ is expressed as

$$[S]_e = \int_{\Omega_e} \frac{1}{\mu_r} \frac{s}{3V} \begin{bmatrix} -\vec{t}_{2,3} \\ \vec{t}_{1,3} \\ -\vec{t}_{1,2} \\ -\vec{t}_{0,3} \\ \vec{t}_{0,2} \\ -\vec{t}_{0,1} \end{bmatrix} \cdot [-\vec{t}_{2,3} \quad \vec{t}_{1,3} \quad -\vec{t}_{1,2} \quad -\vec{t}_{0,3} \quad \vec{t}_{0,2} \quad -\vec{t}_{0,1}] \frac{s}{3V} d\Omega$$

$$= \frac{1}{9\mu_r V} \begin{bmatrix} \vec{t}_{2,3} \cdot \vec{t}_{2,3} & & & & & \\ -\vec{t}_{1,3} \cdot \vec{t}_{2,3} & \vec{t}_{1,3} \cdot \vec{t}_{1,3} & & & & \\ \vec{t}_{1,2} \cdot \vec{t}_{2,3} & -\vec{t}_{1,2} \cdot \vec{t}_{1,3} & \vec{t}_{1,2} \cdot \vec{t}_{1,2} & & & \\ \vec{t}_{0,3} \cdot \vec{t}_{2,3} & -\vec{t}_{0,3} \cdot \vec{t}_{1,3} & \vec{t}_{0,3} \cdot \vec{t}_{1,2} & \vec{t}_{0,3} \cdot \vec{t}_{0,3} & & \\ -\vec{t}_{0,2} \cdot \vec{t}_{2,3} & \vec{t}_{0,2} \cdot \vec{t}_{1,3} & -\vec{t}_{0,2} \cdot \vec{t}_{1,2} & -\vec{t}_{0,2} \cdot \vec{t}_{0,3} & \vec{t}_{0,2} \cdot \vec{t}_{0,2} & \\ \vec{t}_{0,1} \cdot \vec{t}_{2,3} & -\vec{t}_{0,1} \cdot \vec{t}_{1,3} & \vec{t}_{0,1} \cdot \vec{t}_{1,2} & \vec{t}_{0,1} \cdot \vec{t}_{0,3} & -\vec{t}_{0,1} \cdot \vec{t}_{0,2} & \vec{t}_{0,1} \cdot \vec{t}_{0,1} \end{bmatrix} \tag{18}$$

Also, the matrix $[T]_e$ can be written as

$$[T]_e = \int_{\Omega_e} \epsilon_r \begin{bmatrix} \vec{w}_{0,1} \\ \vec{w}_{0,2} \\ \vec{w}_{0,3} \\ \vec{w}_{1,2} \\ \vec{w}_{1,3} \\ \vec{w}_{2,3} \end{bmatrix} \cdot [\vec{w}_{0,1} \quad \vec{w}_{0,2} \quad \vec{w}_{0,3} \quad \vec{w}_{1,2} \quad \vec{w}_{1,3} \quad \vec{w}_{2,3}] \, d\Omega$$

$$= \frac{\epsilon_r}{180V} \begin{bmatrix} 2(I_{00} - I_{01} + I_{11}) & & & & & & \\ I_{00} - I_{01} - I_{02} + 2I_{12} & 2(I_{00} - I_{02} + I_{22}) & & & & & \\ I_{00} - I_{01} - I_{03} + 2I_{12} & I_{00} - I_{02} - I_{03} + 2I_{23} & 2(I_{00} - I_{03} + I_{33}) & & & & \\ I_{01} - I_{11} - 2I_{02} + I_{12} & 2I_{01} - I_{12} - I_{02} + I_{22} & I_{01} - I_{13} - I_{02} + I_{23} & 2(I_{11} - I_{12} + I_{22}) & & & \\ I_{01} - I_{11} - 2I_{03} + I_{13} & I_{01} - I_{12} - I_{03} + I_{23} & 2I_{01} - I_{13} - I_{03} + I_{33} & I_{11} - I_{12} - I_{13} + 2I_{23} & 2(I_{11} - I_{13} + I_{33}) & & \\ I_{02} - I_{12} - I_{03} + I_{13} & I_{02} - I_{22} - 2I_{03} + I_{23} & 2I_{02} - I_{23} - I_{03} + I_{33} & I_{12} - I_{22} - 2I_{13} + I_{23} & 2I_{12} - I_{23} - I_{13} + I_{33} & 2(I_{22} - I_{23} + I_{33}) & \end{bmatrix} \tag{19}$$

where $I_{ij} = \vec{A}_i \cdot \vec{A}_j$.

3.2 *Transformed Generalized Eigenmatrix Equation*

The stationary points of the functional $F(\vec{E})$ in (9) correspond to the solutions of the following generalized eigenmatrix equation

$$[S]e = k^2[T]e. \tag{20}$$

Note that the global matrices $[S]$ and $[T]$ are semi-definite and positive-definite real-symmetric matrices, respectively. Despite their sparse nature, the dimension of the generalized eigenmatrix equation is large and, hence, only iterative methods can be used to solve (20). The Lanczos algorithm [11] has been used, with much success, to solve symmetric generalized eigenmatrix equations. However, since in (20) the more dominant mode corresponds to smaller eigenvalue k^2, the direct application of the Lanczos algorithm may converge rather slowly. This problem can be circumvented, however, and a computationally efficient algorithm can be derived by rewriting (20). To this end, we first find an estimate k_g^2, the lower bound of the physical modes, which can be approximated from the largest dimension and the material properties inside the cavity. We then rewrite (20) as

$$[A]x = \lambda[B]x \tag{21}$$

where $[A] = [T]$, $\lambda = (1/k^2 + k_g^2)$ and $[B] = [S] + k_g^2[T]$. The advantage of using (21) is that, except for the null vectors of the curl operator, the more dominant modes correspond to the larger eigenvalues of this equation. Due to the nature of the Krylov subspace iteration, the larger eigenpairs almost always converge faster. Therefore, by rearranging the generalized eigenmatrix equation into (21), the resonant modes of the cavity can be computed more or less in the order of dominance.

The convergence of the Lanczos algorithm for the dominant mode, with $k^2 \neq 0$, can be improved drastically by selecting an initial vector which is orthogonal to the null ($k^2 = 0$) eigenpairs [14].

IV. Convergence Study

One criterion for the acceptability of a numerical algorithm is its rate of convergence. For a FEM implementation, this rate can be estimated in two ways, viz., from the numerical theories and from systematic numerical experiments. Theoretically, the rate of convergence is a consequence of the consistency and stability analyses [12]. The consistency and stability analyses of present approach for modeling three-dimensional cavities will be reported in a later paper. In this section, we present a method for obtaining the rate of convergence for un-structured tetrahedral meshes through numerical experiments.

To be able to conduct a systematic convergence study of FEM on tetrahedral meshes, we need to generate sim-

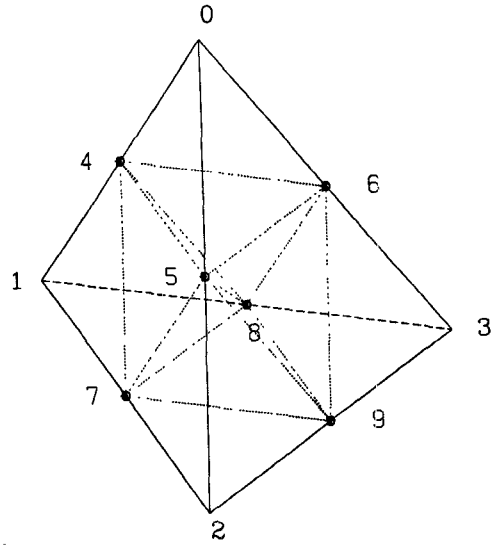

Fig. 2. A *factor-of-two mesh division.*

ilar but finer meshes by subdividing a coarse one. Fig. 2 shows a mesh division of a tetrahedron into eight smaller tetrahedra. We call such a scheme "*factor-of-two mesh refinement.*" In general, the eight smaller tetrahedra generated from The "*factor-of-two mesh refinement*" do not completely resemble the original tetrahedron. For the practical application, however, the finer mesh obtained by using the "*factor-of-two mesh refinement*" does provide a satisfactory similarity to the original mesh. The following table summarizes the "*factor-of-two mesh refinement:*"

$$\text{tetra } \{0, 1, 2, 3\} \Rightarrow \begin{matrix} \text{tetra } \{0, 4, 5, 6\} \\ \text{tetra } \{1, 4, 7, 8\} \\ \text{tetra } \{2, 5, 7, 9\} \\ \text{tetra } \{3, 6, 8, 9\} \\ \text{tetra } \{4, 5, 6, 8\} \\ \text{tetra } \{4, 5, 7, 8\} \\ \text{tetra } \{5, 7, 8, 9\} \\ \text{tetra } \{5, 6, 8, 9\} \end{matrix} \tag{22}$$

The test geometry of the experiment is an air-filled rectangular cavity with dimensions 1 m × 2 m × 2 m, as shown in Fig. 3, and the TE_{101} mode is dominant with a resonant frequency of $f_0 = 106.066$ MHz. The experiment starts with a very coarse tetrahedral mesh, and defines the cell size $h = 1$. The "*factor-of-two mesh refinement*" is then used to generate finer meshes with $h = \frac{1}{2}$, $h = \frac{1}{4}$, etc. For each tetrahedral mesh, we compute the resonant frequency of the cavity using the procedure outlined above and then calculate the relative error to the exact resonant frequency. The result is shown in Fig. 4. The convergence is governed by $\epsilon \propto h^n$, where ϵ is the relative error and n is the value of the index to be determined, i.e., the rate of convergence. From Fig. 4, we see

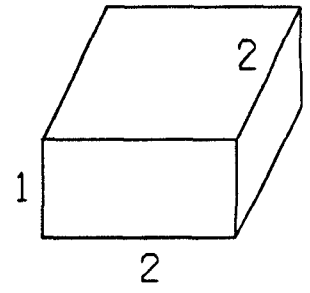

Fig. 3. An air-filled rectangular cavity.

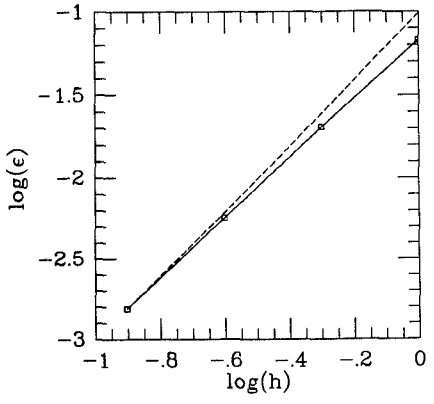

Fig. 4. Plot of the relative error of the numerical result versus the cell size for the cavity in Fig. 3.

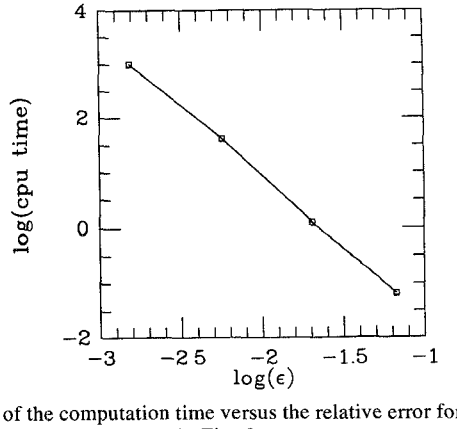

Fig. 5. Plot of the computation time versus the relative error for the cavity in Fig. 3.

that the index n is very close to 2. This leads us to conclude that the use of the edge elements yields a second-order accuracy. This is not surprising, however, since the resonant frequency is a variational quantity in the functional (9) and, therefore, it often offers better accuracy than the computed vector fields $\vec{E}$ and $\vec{H}$. We should also point out that the second-order accuracy for computing the resonant frequency is only valid for cavity mode whose field distribution is smooth. For cavities that have re-entrant points, as described in [12], the convergence rate is expected to be worse.

A plot of the computation time vs. the accuracy is provided in Fig. 5. From Fig. 5, we see that, once again, the slope is very close to 2. This can be explained as follows. To apply the Lanczos algorithm for the solution of a gen-

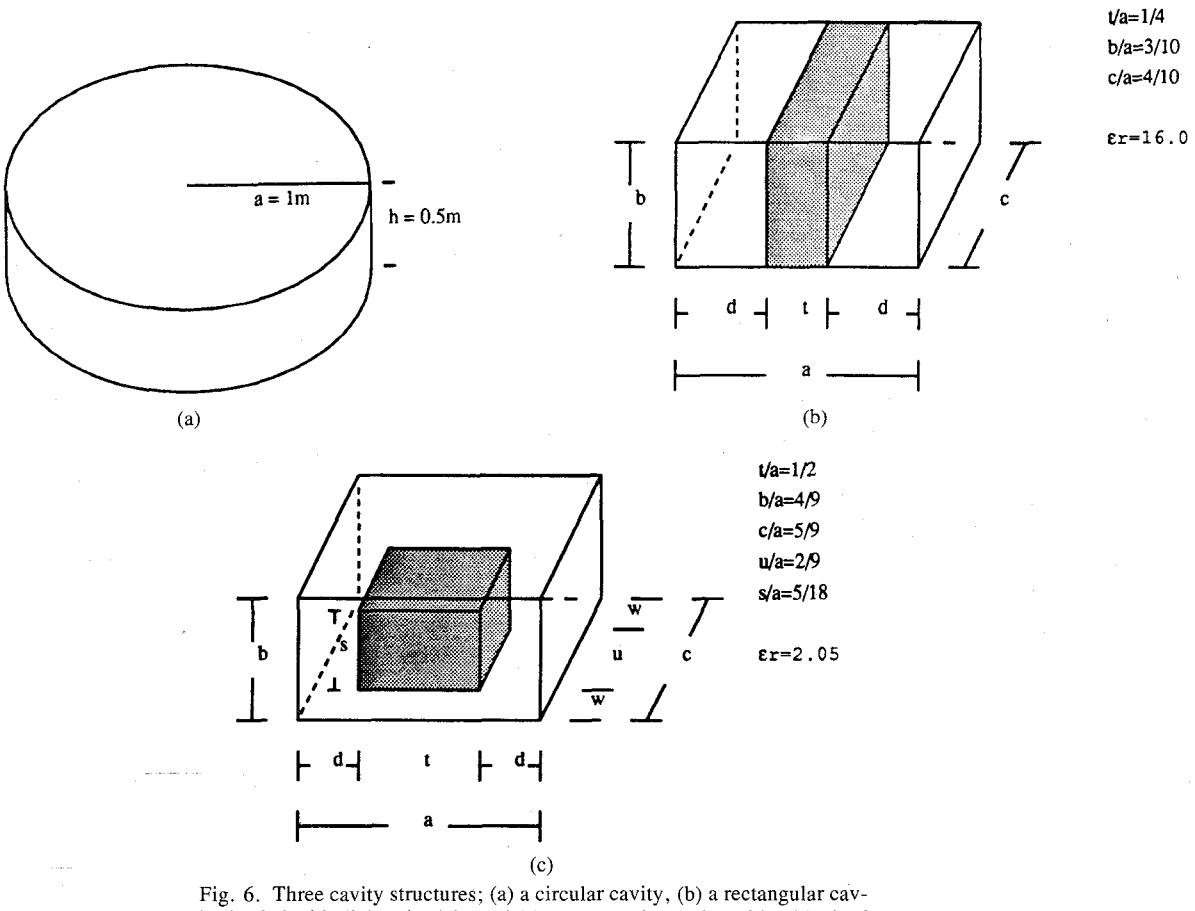

Fig. 6. Three cavity structures; (a) a circular cavity, (b) a rectangular cavity loaded with dielectric slab, and (c) a rectangular cavity with a block of dielectric.

eralized eigenmatrix equation (21), each iteration step involves the solution of a matrix equation of the form

$$v = [B]^{-1}y \tag{23}$$

where v is the updated Krylov vector generated through iteration upon y. Since $[B]$ is a positive-definite matrix, we have used the Polynomial-Preconditioned Conjugate Gradient (PPCG) [13] method to solve the matrix equation efficiently. Therefore, the total computation time of present approach can be written as

$$\text{cpu time} \propto l \times T \tag{24}$$

where l is the number of iterations in the Lanczos algorithm, and T is the computer time to solve (23) using PPCG method. In general, the number of iterations l would be expected to increase with the refinement of the mesh. However, we found in this study that, l changes relatively little with the increase in the mesh density. As a result, the matrix solution time T increases as

$$T \propto N^{1.333} \tag{25}$$

for finer meshes, where N is the degrees of freedom. Furthermore, in three dimensions, we have $N \propto h^3$. Based on above discussions and the fact that $\epsilon \propto h^2$, we finally arrive at the conclusion that

$$\text{cpu time} \propto \epsilon^2. \tag{26}$$

V. Numerical Results

A general finite-element computer program has been written to implement the numerical procedure presented in this paper and, the transformed generalized eigenmatrix equation has been solved by using the Lanczos algorithm.

To validate the current approach, numerical results for a circular cavity, a rectangular cavity loaded with dielectric slab, and a rectangular cavity containing a rectangular block of dielectric have been tested. The geometries and the material properties of these three cavities are shown in Fig. 6. Table I summarizes the numerical results. From Table I, we note that accurate resonant frequencies (within 1% error) are obtained for various cavity structures with at most 30 seconds of cpu time on a Decstation 5000/200 machine. We also note from Table I that, it takes a much longer time to compute the resonance of the circular cavity than it does for the rectangular one. This is owing to the fact that many triangular patches are needed to accurately represent a curved surface. Consequently, the degrees of freedom needed to model the structure in Fig. 6(a) is considerably larger than those required in Fig. 6(b) and (c).

TABLE I
NUMERICAL RESULTS WITH COMPARISONS TO EXACT OR MEASURED VALUES FOR THREE CAVITIES IN FIG. 6

Geometry	*ka* Exact or Measured Value	*ka* Computed	Relative Error (%)	cpu Time (seconds)
Fig. 6(a)	2.405	2.429	1.02	29.05
Fig. 6(b)	2.5829	2.59413	0.4348	0.65
Fig. 6(c)	5.22[Albani]	5.159	1.167	1.16

VI. CONCLUSIONS

A new vector finite element approach for solving electromagnetic problems, which is based on the use of edge elements, has been presented in this paper. The element matrices for edge-elements for analyzing three-dimensional cavity structures have been derived. By expressing the entries in the element matrices in terms of geometric quantities, the edge-elements approach can be readily applied to many other engineering applications.

We have also conducted a numerical experiment to determine the rate of convergence of using the edge-elements to compute the dominant resonant frequency of a rectangular cavity. Although, the vector field is approximated within each tetrahedron by an incomplete first-order polynomial, the computed resonant frequency is found to be second-order accurate because of its variational nature.

ACKNOWLEDGMENT

The authors would like to thank Dr. Shirley Min for her help received during the course of this work. We also thank the reviewers for making many valuable suggestions to improve the quality of the paper.

REFERENCES

[1] S. Akhtarzad and P. B. Johns, "Solution of Maxwell's equations in three space dimensions and time by the t.l.m. method of numerical analysis," *Proc. Inst. Elec. Eng.*, vol. 122, pp. 1344–1348, Dec. 1975.

[2] M. Albani and P. Bernardi, "A numerical method based on the discretization of Maxwell's equations in integral form," *IEEE Trans. Microwave Theory Tech.*, MTT-22, pp. 446–450, Apr. 1974

[3] J. P. Webb, G. L. Maile, and R. L. Ferrari, "Finite-element solution of three-dimensional electromagnetic problems," *Proc. Inst. Elec. Eng., Pt. H*, 130, pp. 153–159, Mar. 1983.

[4] J. P. Webb, "The finite-element method for finding modes of dielectric-loaded cavities," *IEEE Trans. Microwave Theory and Tech.*, MTT-33, pp. 635–639, July 1985.

[5] B. M. A. Rahman and J. B. Davies, "Finite-element analysis of optical and microwave waveguide problems," *IEEE Trans. Microwave Theory Tech.*, MTT-32, pp. 20–28, Jan. 1984.

[6] A. J. Kobelansky and J. P. Webb, "Eliminating spurious modes in finite-element waveguides problems by using divergence-free fields," *Electron. Lett.*, vol. 22, pp. 569–570, 1986.

[7] A. Bossavit, "Simplicial finite elements for scattering problems in electromagnetism," *Computer Methods in Applied Mechanics and Engineering*, vol. 76, pp. 299–316, 1989.

[8] J. Wang and N. Ida, "Eigenvalue analysis in EM cavities using divergence-free finite elements," in *Proc. Fourth Biennial IEEE Conf. on Electromagnetic Field Computation*, Toronto, Canada, 1990.

[9] M. Hano, "Finite-element solution of three-dimensional resonator problems. Novel rectangular parallelepiped elements," *Electronics and Communications in Japan*, part 2, vol. 71, pp. 27–34, 1988.

[10] R. F. Harrington, *Time Harmonic Electromagnetic Fields*. New York: McGraw-Hill, 1961.

[11] B. N. Parlett, *The Symmetric Eigenvalue Problem*. Englewood Cliffs, NJ: Prentice-Hall, 1980.

[12] G. Strang and G. J. Fix, *An Analysis of the Finite Element Method*. Englewood Cliffs, NJ: Prentice Hall, 1973.

[13] G. H. Golub and C. F. V. Loan, *Matrix Computations*. Baltimore, MD: Johns Hopkins University Press, 2nd ed., 1989, pp. 534.

[14] J. F. Lee, D. K. Sun, and Z. J. Cendes, "Full-wave analysis of dielectric waveguides using tangential vector finite elements," *IEEE Trans. Microwave Theory Tech.*, vol. 39, pp. 1262–1271, Aug. 1991.

Jin-Fa Lee (M'88) was born in Taipei, Taiwan, in 1960. He received the B.S. degree from National Taiwan University, in 1982 and the M.S. and Ph.D. degrees from Carnegie Mellon University in 1986 and 1989, respectively, all in electrical engineering.

From 1988 to 1990, he was with ANSOFT Corp., where he developed several CAD/CAE finite element programs for modeling three-dimensional microwave and millimeter-wave circuits. From 1990 to 1991, he was a post-doctoral fellow at the Electromagnetic Communication Laboratory, University of Illinois at Urbana-Champaign. Currently, he is an assistant professor at Department of Electrical Engineering, Worcester Polytechnic Institute.

Dr. Lee's current research interests are: analyses of numerical methods, couplintgs of active and passive components in high-speed electronic circuits, solution of the moving boundary problem and its application to semiconductor process modelings, and EM field propagation in linear and/or non-linear medium.

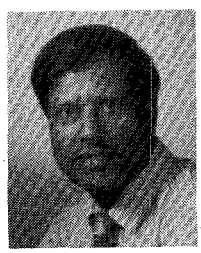

Raj Mittra (S'54–M'57–SM'69–F'71) is Director of the Electromagnetic Communication Laboratory of the Electrical and Computer Engineering Department and Research Professor of the Coordinate Science Laboratory at the University of Illinois. He is a former president of AP-S, and he has served as the editor of the IEEE TRANSACTIONS ON ANTENNAS AND PROPAGATION. He is president of RM Associates, a consulting organization providing services to several industrial and governmental organizations.

Dr. Mittra's professional interests include the areas of analytical and computer-aided electromagnetics, high-speed digital circuits, radar scattering, satellite antennas, microwave and millimeter-wave integrated circuits, frequency selective surface, EMP and EMC analysis, and remote sensing.